

# Knock-on Tail Formation Due to Nuclear Elastic Scattering and Its Observation Method Using $\gamma$ -Ray-Generating ${}^6\text{Li}+\text{d}$ Reaction in Tokamak Deuterium Plasmas<sup>\*</sup>)

Hideaki MATSUURA, Shota SUGIYAMA, Shogo KAJIMOTO, Daisuke SAWADA,  
Yosuke NISHIMURA and Yasuko KAWAMOTO

*Department of Applied Quantum Physics and Nuclear Engineering,  
Kyushu University, Motoooka, Fukuoka 819-0395, Japan*

(Received 8 January 2016 / Accepted 1 June 2016)

A knock-on tail formation in deuteron velocity distribution function due to nuclear elastic scattering (NES) by energetic protons and its observation method using  $\gamma$ -ray-generating  ${}^6\text{Li}(\text{d},\text{p}){}^7\text{Li}$  reaction are examined for proton-beam-injected deuterium plasmas. The proton velocity distribution function is obtained by means of the ion trajectory analysis in a Tokamak magnetic configuration. The knock-on tail in two-dimensional (2D) deuteron velocity distribution function due to NES by energetic protons is evaluated via Boltzmann collision integral and 2D Fokker-Planck simulation. From the 2D deuteron velocity distribution function obtained, enhancement of the emission rate of 0.48-MeV  $\gamma$ -rays by  ${}^6\text{Li}(\text{d},\text{p}){}^7\text{Li}^*$ ,  ${}^7\text{Li}^*\rightarrow{}^7\text{Li}+\gamma$  reaction due to NES is evaluated. It is shown that the  $\gamma$ -ray emission rate is significantly influenced by the magnitude of the knock-on tail, and the  $\gamma$ -ray-generating reaction can be a useful tool for the knock-on tail observation.

© 2016 The Japan Society of Plasma Science and Nuclear Fusion Research

Keywords: nuclear elastic scattering, knock-on tail,  $\gamma$ -ray-generating  ${}^6\text{Li}(\text{d},\text{p}){}^7\text{Li}$  reaction, Boltzmann collision integral, Fokker-Planck equation

DOI: 10.1585/pfr.11.1403105

## 1. Introduction

It is well known that in a thermonuclear plasma energetic ions create knock-on tails [1, 2] in fuel-ion velocity distribution functions due to nuclear elastic scattering (NES) [3, 4]. In deuterium-tritium (DT) thermonuclear plasmas, 3.52-MeV  $\alpha$ -particles are continuously produced, and use of beam injection with energy more than 1 MeV is considered. In such a case, NES effects on slowing down of energetic ions would not be negligible compared with those due to Coulomb collisions. We have evaluated the NES effects on burning plasma properties for several situations that energetic ions exist [5–7], on the basis of the Boltzmann-Fokker-Planck (BFP) analysis model [5, 8–10]. Many calculations have predicted that NES accelerates slowing-down process of fast ions and enhances the fractional energy deposition from fast to bulk ions [11–13]. Especially in  $\text{D}^3\text{He}$  plasmas, it has been predicted that if NES is neglected the fractional transferred energy from fusion-produced protons to bulk ions is underestimated approximately one third compared with the energy when NES is considered [12, 13]. By considering the NES effect, the confinement condition can also be significantly influenced [13, 14]. Recently we have also shown that the magnitude of the energetic component in proton slowing-down distri-

bution in  $\text{D}^3\text{He}$  plasmas is considerably overestimated if NES is neglected [15]. When population of the energetic ion component is modified, plasma heating properties may also be modified. The contributions of NES can determine the essential physics of thermonuclear fusion especially in  $\text{D}^3\text{He}$  plasmas, and it is important to experimentally ascertain the knock-on tail formation to construct the database for NES effect on the plasma burning properties.

So far we have considered the scenarios to examine the NES effect in a deuterium plasma [16–18]. In this paper, we focus our attention on a verification scenario of knock-on tail formation using 0.48-MeV  $\gamma$ -rays by  ${}^6\text{Li}(\text{d},\text{p}){}^7\text{Li}^*$ ,  ${}^7\text{Li}^*\rightarrow{}^7\text{Li}+\gamma$  reaction [19–22] in a deuterium plasma. In Fig. 1 the cross section of the  ${}^6\text{Li}(\text{d},\text{p}){}^7\text{Li}$  reaction is shown as a function of the relative energy of reactants. The cross section rapidly increases with increasing relative energy. Owing to the existence of small fraction of knock-on tail component, “velocity-averaged”  ${}^6\text{Li}(\text{d},\text{p}){}^7\text{Li}$  reaction rate coefficient would be significantly influenced. It is expected that by using the  $\gamma$ -ray-generating reaction for various plasma conditions, we can quantitatively estimate the magnitude of the knock-on tail. We consider the knock-on tail in deuteron velocity distribution function by energetic protons in proton-beam-injected deuterium plasmas. Previously we roughly evaluated the  ${}^6\text{Li}(\text{d},\text{p}){}^7\text{Li}$  reaction rate coefficient assuming a uniform plasma [16]. In this paper we develop more

author's e-mail: mat@nucl.kyushu-u.ac.jp

<sup>\*</sup>) This article is based on the invited talk at the 32nd JSPF Annual Meeting (2015, Nagoya).

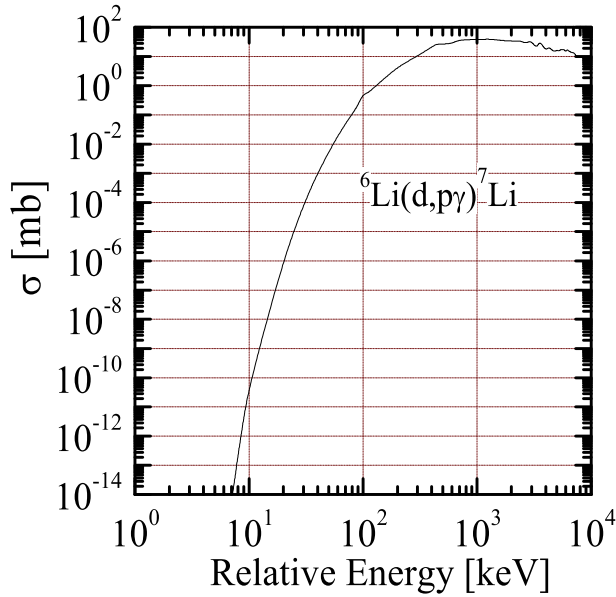


Fig. 1  ${}^6\text{Li}(d,p){}^7\text{Li}$  cross section as a function of relative energy [19–22].

precise model heading on the future experiment and re-evaluate the rate coefficient of the  $\gamma$ -ray-generating reaction. We take into account behaviors of beam-injected protons in a magnetic confinement device by means of the ion trajectory analysis. Using the obtained two-dimensional (2D) velocity distribution function of beam-injected protons, velocity distribution of the deuteron knock-on source due to NES by energetic protons is evaluated in 2D velocity space from Boltzmann collision integral at every position in a fusion plasma. From the 2D deuteron velocity distribution function, which is obtained by solving 2D Fokker-Planck (FP) equation, enhancement of the 0.48-MeV  $\gamma$ -rays emission rate due to NES is evaluated. We first show the result when a point proton source in a plasma due to NBI (which implies that all of the injected hydrogens are ionized at a spatial point in the plasma as a monoenergetic beam) is assumed. By superposing the results of the point source, the results when actual ionization profile is considered are shown. The purpose of this study is to show a possibility of the  $\gamma$ -ray-generation reaction to verify the knock-on tail formation due to NES on the basis of a newly-developed more precise model.

## 2. Analysis Model

### 2.1 Evaluation of proton velocity distribution function

To estimate the proton distribution function in a Tokamak device, ion trajectory analysis is carried out. The simulation is made by using ORBIT code [23]. We assume ITER-like magnetic configuration as shown in Fig. 2. The equilibrium flux surfaces are determined according to the model developed by Yavorskij, *et al.* [24]. The pa-

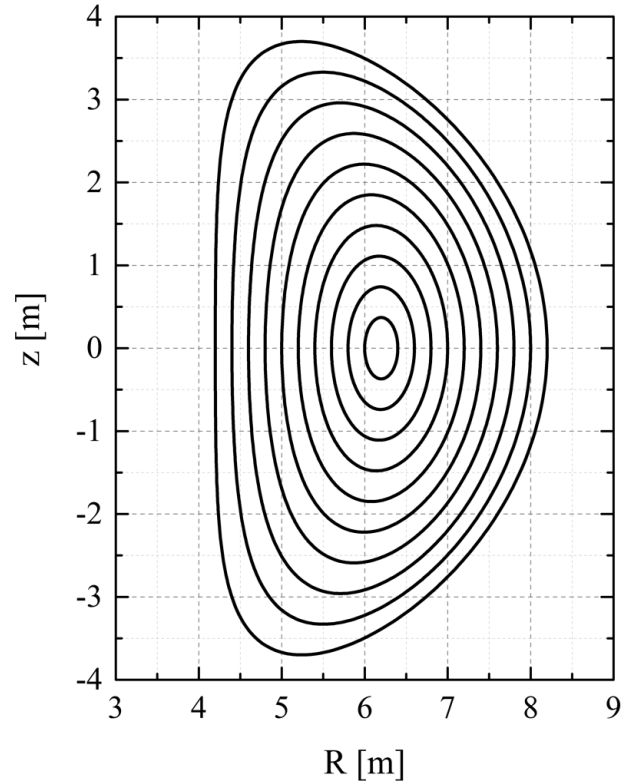


Fig. 2 Magnetic flux surface assumed in the calculation [24].

Table 1 Calculation parameters for a ITER-like Tokamak plasma.

Parameter	Value
$B_t$ [T]	5.3
$R$ [m]	6.2
$a$ [m]	2.0
$\kappa$	1.85
$\delta$	0.48

rameters to describe the flux surfaces and plasma conditions assumed throughout the calculations are shown in Table 1. Radial profiles of temperature, ion and electron densities are assumed as  $T(r) = T(0) \times (1 - (r/a)^2)$  and  $n_j(r) = n_j(0) \times (1 - (r/a)^2)^{0.05}$  ( $j = d, e, {}^6\text{Li}$ ) respectively [25]. Radial profile of the safety factor assumed in the simulations is referred from the work of Green [25], which is obtained for ITER plasma (see Fig. 3). The calculation to simulate the proton behaviors in the proton beam-injected deuterium plasma follows 24,000 proton orbits for 170,000~840,000 toroidal transit time, i.e., 1.5~3.3 sec,

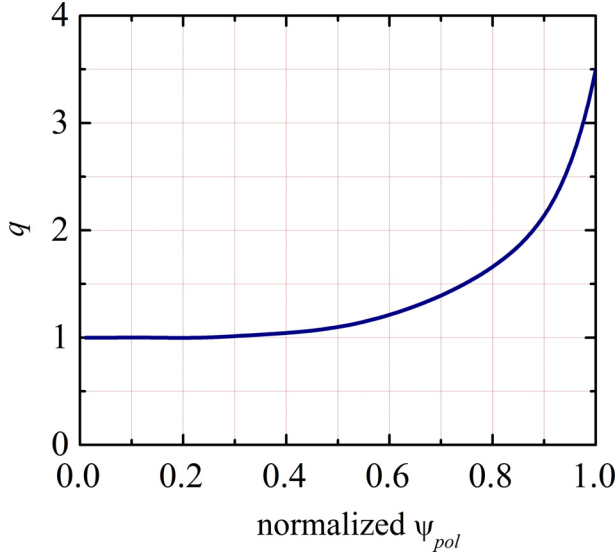


Fig. 3 Radial profile of the safety factor [25].

depending on beam-injection energy. By gathering the information of each proton velocity, the distribution function of proton is evaluated at each position in a Tokamak plasma.

## 2.2 Evaluation of knock-on source for deuterons

The bulk deuterons are knocked up by energetic protons due to NES and moved from thermal to higher energy range. We next evaluate the knocked up distribution (knock-on source) for deuterons. For this purpose the following Boltzmann collision integral is carried out using the previously obtained proton distribution function.

$$S_d^{\text{NES}}(\vec{v}_d) = \iint f_d(\vec{v}'_d) f_p(\vec{v}_p) P(\vec{v}'_d \rightarrow \vec{v}_d | \vec{v}_p) v'_r \sigma_{\text{NES}}(v'_r) d\vec{v}_p d\vec{v}'_d, \quad (1)$$

where  $\sigma_{\text{NES}}$  is the cross section of NES. The data are taken from the work by Perkins and Cullen [4]. Here  $v'_r = |\vec{v}_p - \vec{v}'_d|$ .  $P$  represents the probability that a deuteron velocity is changed from  $\vec{v}'_d$  to  $\vec{v}_d$  as a result of a collision with an energetic proton which has velocity  $\vec{v}_p$  in the laboratory system. The schematic view of the change of the deuteron velocities before and after the collision is shown in Fig. 4. Here  $\vec{V}'_d$  and  $\vec{V}_d$  represent the deuteron velocities in the center-of-mass system before and after the collision respectively, and  $\vec{v}_c$  is the center-of-mass velocity. Because the absolute value of  $\vec{V}'_d$  does not change during the collision,  $\vec{V}_d$  is always on the surface of the sphere which has radius  $|\vec{V}'_d|$  with the center at the end of vector  $\vec{v}_c$ . We have determined the probability  $P(\vec{v}'_d \rightarrow \vec{v}_d | \vec{v}_p)$  by using the random numbers for angle of scattering in the center-of-mass system  $\phi$  and angle  $\xi$  around the axis along with  $\vec{v}_c$ . In this study we assume isotropic scattering in the center-of-mass

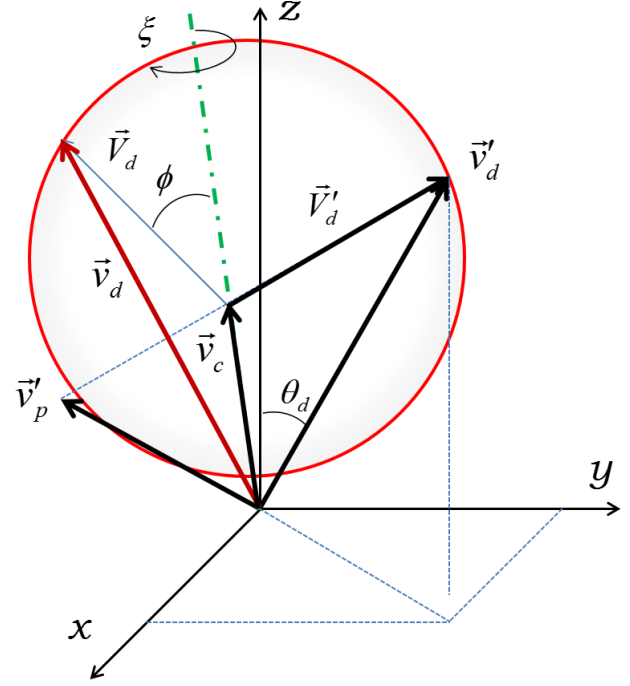


Fig. 4 Schematic view of the change in the deuteron velocities before and after NES.

system. The integration of Eq. (1) is made for all combinations of  $\vec{v}'_d$  and  $\vec{v}_p$ , and the knocked up deuteron distribution in the velocity space is obtained as a function of  $\vec{v}_d$ . In this process the deuteron distribution function is assumed to be Maxwellian.

## 2.3 Evaluation of deuteron velocity distribution function

The equilibrium deuteron distribution function  $f_d(v, \mu)$  is obtained by solving the following 2D FP equation;

$$\left( \frac{\partial f_d}{\partial t} \right)^{\text{Coulomb}} + \frac{1}{v^2} \frac{\partial}{\partial v} \left( \frac{v^3}{2\tau_c^*(v)} \right) f_d(v, \mu) + S_d^{\text{NES}}(v, \mu) - \frac{f_d(v, \mu)}{\tau_p^*(v)} = 0. \quad (2)$$

Here  $\mu$  is the direction cosine in the spherical coordinate. The first term of Eq. (2) represents the influence of the Coulomb collisions with background particles, i.e. deuteron,  ${}^6\text{Li}$  and electron.

$$\left( \frac{\partial f}{\partial t} \right)^{\text{Coulomb}} = \frac{1}{v^2} \frac{\partial}{\partial v} \left[ \varphi f + \frac{\varphi T_j}{m_d v} \frac{\partial f}{\partial v} \right] + \frac{\psi}{2v^3} \frac{\partial}{\partial \mu} \left[ (1 - \mu^2) \frac{\partial f}{\partial \mu} \right]. \quad (3)$$

When background particles are assumed to be Maxwellian,

$$\varphi = \Gamma_d \sum_j n_j \left( \frac{Z_j}{Z_d} \right)^2 \frac{m_d}{m_j} \left[ \Phi(X_j) - \frac{2}{\sqrt{\pi}} X_j \exp(-X_j^2) \right], \quad (4)$$

$$\psi = \Gamma_d \sum_j n_j \left( \frac{Z_j}{Z_d} \right)^2 \frac{1}{X_j^2} \left[ \frac{2}{\sqrt{\pi}} X_j \exp(-X_j^2) - (1 - 2X_j^2) \Phi(X_j) \right], \quad (5)$$

where subscript  $j$  represents the background charged particles, i.e., deuteron,  ${}^6\text{Li}$  and electron,  $\Phi$  is the error function,  $X_j = \sqrt{m_j/2T}v$  and  $\Gamma_d = e^4 \ln \Lambda / 4\pi\epsilon_0^2 m_d^2$ .

The second term in the left-hand side of Eq. (2) represents the diffusion in velocity space due to thermal conduction. In this paper unknown loss mechanism has been incorporated into the analysis by using dimensionless parameter  $\gamma$  following Bittoni's treatment [26], i.e.,  $\tau_C^*(v) = C_C \tau_C$ ,  $\tau_P^*(v) = C_P \tau_P$  (when  $v < v_{th}$ ) and  $\tau_C^*(v) = C_C \tau_C (v/v_{th})^\gamma$ ,  $\tau_P^*(v) = C_P \tau_P (v/v_{th})^\gamma$  (when  $v \geq v_{th}$ ). Here  $v_{th}$  represents the thermal velocity of deuteron and the coefficient  $C_C(C_P)$  is determined so that the velocity-integrated energy (particle) loss rate becomes  $(3/2)n_d T / \tau_C$  ( $n_d / \tau_P$ ). The high exponent  $\gamma$  chosen ensures rapid increment of both energy and particle confinement times in high energy range compared with the ones in the thermal energy range. In this paper throughout the calculations  $\gamma = 4$  is assumed. As was discussed in Ref. [5], for the present study the  $\gamma$  is not an influential parameter. Considering both energy loss mechanisms due to thermal conduction and particles transport loss from the plasma, the confinement time due to conduction loss  $\tau_C$  is determined for each ion species using the global energy confinement time  $\tau_E$  so that the following relation is satisfied for each species,

$$\frac{(3/2)n_d T}{\tau_E} = \frac{(3/2)n_d T}{\tau_C} + \int \frac{(1/2)m_d v^2}{\tau_P^*(v)} f_d(v, \mu) d\vec{v}. \quad (6)$$

## 2.4 Evaluation of ${}^6\text{Li}(d, p\gamma){}^7\text{Li}$ reaction rate coefficient

The 0.48-MeV  $\gamma$ -ray emission rate is proportional to the  ${}^6\text{Li}(d, p\gamma){}^7\text{Li}$  reaction rate coefficient. From the obtained deuteron velocity distribution function, the  ${}^6\text{Li}(d, p\gamma){}^7\text{Li}$  reaction rate coefficient is evaluated as

$$\langle \sigma v \rangle_{6\text{Li}+d} = \iint f_d(\vec{v}_d) f_{6\text{Li}}(\vec{v}_{6\text{Li}}) v_r \sigma_{6\text{Li}+d}(v_r) d\vec{v}_{6\text{Li}} d\vec{v}_d. \quad (7)$$

Here  $v_r = |\vec{v}_d - \vec{v}_{6\text{Li}}|$ . The  ${}^6\text{Li}$  distribution function is assumed to be Maxwellian. The cross section of  ${}^6\text{Li}(d, p\gamma){}^7\text{Li}$  reaction shown in Fig. 1 is used for the calculation. Throughout the calculations,  ${}^6\text{Li}$  density is assumed as  $n_{6\text{Li}}(0) = 0.01n_d(0)$ .

## 3. Results and Discussion

A deuterium plasma with proton-beam injection is considered. In Fig. 5 we first show the volume-averaged proton distribution functions for (a) tangential and (b) vertical beam injections as a function of both parallel and

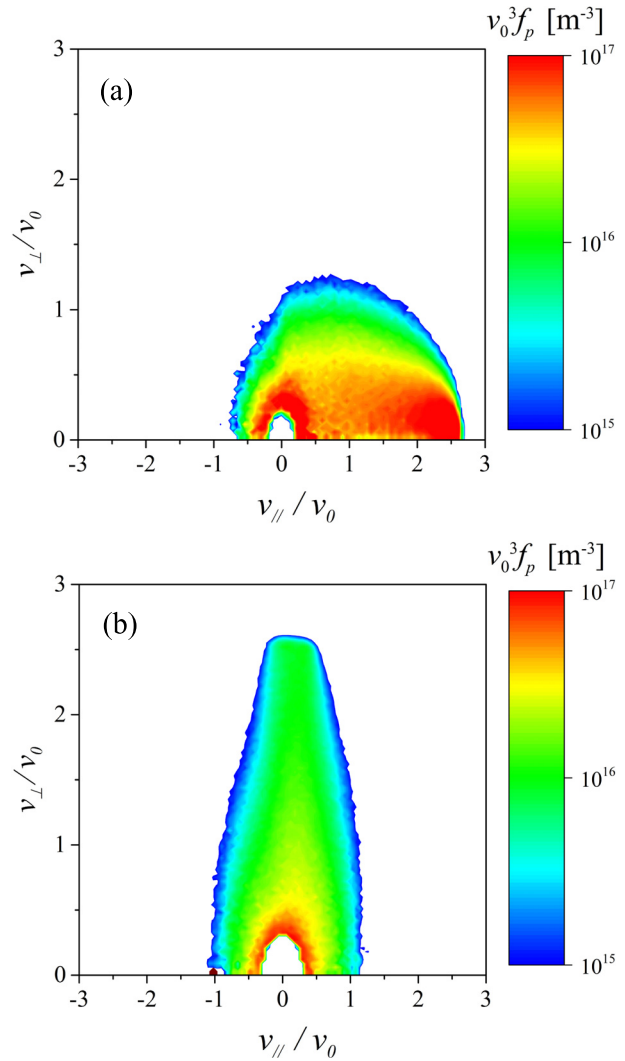


Fig. 5 Volume-averaged proton velocity distribution function for (a) tangential and (b) vertical beam injections with 200 keV beam-injection energy. Deuteron density  $n_d(0) = 10^{19} \text{ m}^{-3}$  and electron temperature  $T_e(0) = 2 \text{ keV}$  are assumed.

vertical velocity components to the toroidal axis. The velocity variable is normalized to the deuteron speed  $v_0 = (2T_0/m_d)^{1/2}$ . Here  $T_0$  is taken as 60 keV. The neutral hydrogen beam is assumed to be ionized on the toroidal axis and energetic protons generate at the ionized place. In the calculation, deuteron density  $n_d(0) = 10^{19} \text{ m}^{-3}$ , electron temperature  $T_e(0) = 2 \text{ keV}$ , energy and particle confinement times  $\tau_E = (1/2)\tau_P = 1 \text{ sec}$ , beam-injection energy and power  $E_{\text{NBI}} = 200 \text{ keV}$ ,  $P_{\text{NBI}} = 33 \text{ MW}$  are assumed. In this study the absolute values of the proton distribution function are determined by comparing the one dimensional (1D) proton distribution function which is obtained by integrating  $f_p(\vec{v}_p)$  for angular coordinates with the analytical solution of FP equation, i.e., so called ‘‘slowing-down distribution’’ [27].

It is found that the non-Maxwellian components are

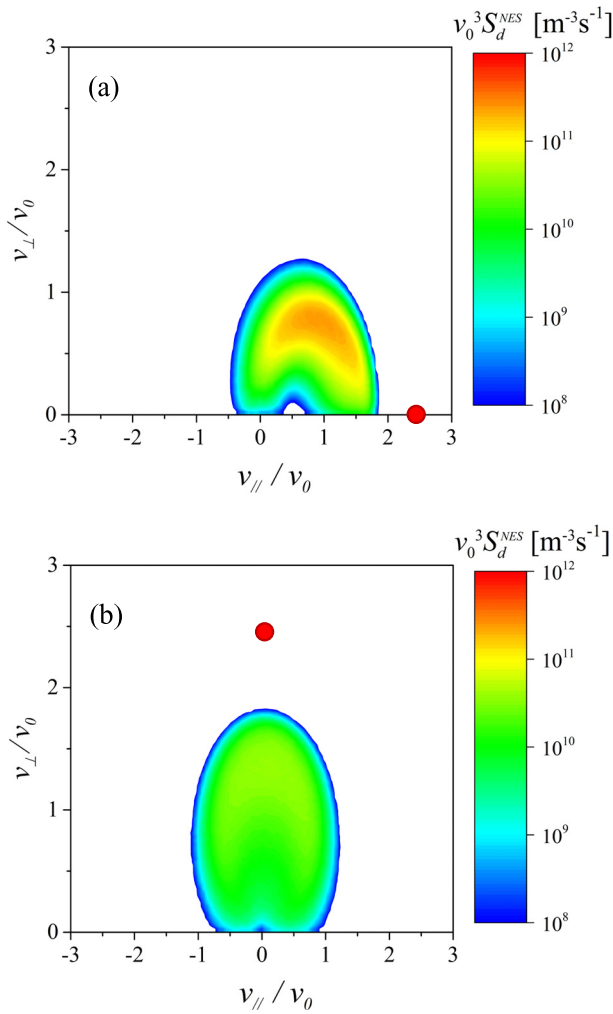


Fig. 6 Volume-averaged distribution functions of knocked up deuterons due to NES by energetic protons for (a) tangential and (b) vertical beam injections with 200 keV beam-injection energy. Deuteron density  $n_d(0) = 10^{19} \text{ m}^{-3}$  and electron temperature  $T_e(0) = 2 \text{ keV}$  are assumed.

formed owing to the energetic beam injection almost along with the beam-injected direction, and the energetic protons slow down toward thermal energy range. In order to thermalize the injected protons perfectly so that Maxwellian component appears, it would be necessary much longer simulation (CPU) time. The purpose of this study, however, is to examine the knock-on tail formation in deuteron velocity distribution function. Because the NES cross section of low energy proton, i.e., less than  $\sim 100 \text{ keV}$ , is considerably small, the distribution function shown in Fig. 5 would be sufficient to examine the knock-on tail formation in deuteron distribution function via NES.

During the slowing-down process, the energetic protons knock up thermal deuterons to higher energy range via NES. The volume-averaged distribution functions of the knocked up deuterons are shown in Fig. 6 for (a) tangential and (b) vertical proton beam injections, i.e., the calculations correspond to Figs. 5 (a) and (b) respectively.

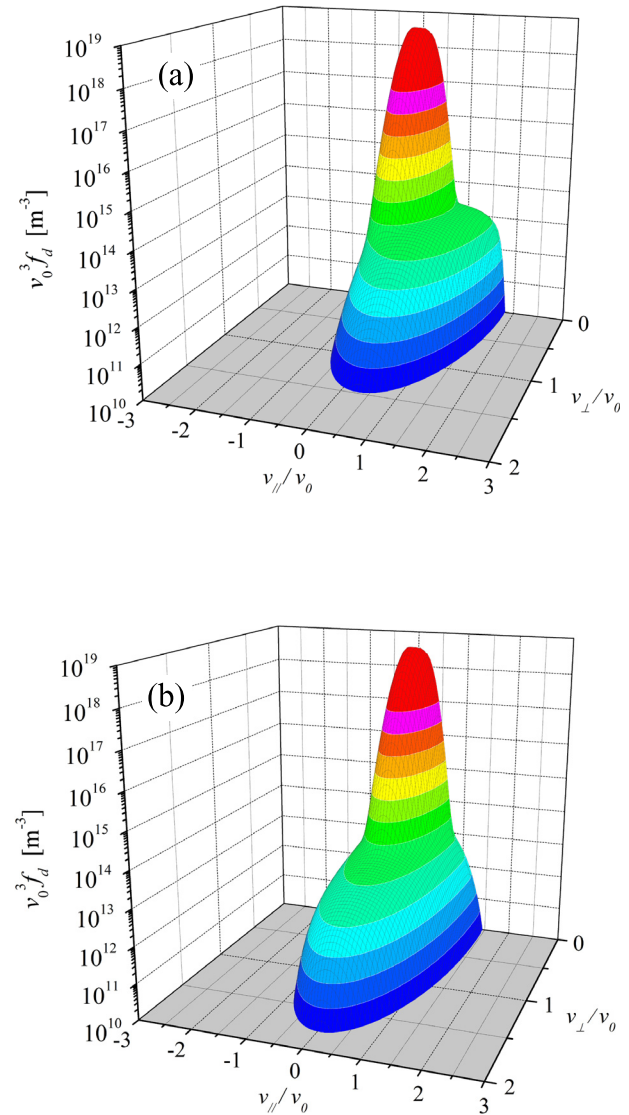


Fig. 7 Volume-averaged deuteron velocity distribution functions for (a) tangential and (b) vertical proton beam injections with 200 keV beam-injection energy. Deuteron density  $n_d(0) = 10^{19} \text{ m}^{-3}$  and electron temperature  $T_e(0) = 2 \text{ keV}$  are assumed.

The red circles indicate beam injection points on the velocity space. In the elastic scattering process, the recoiled ion energy tends to increase when ion is scattered to the same direction as energetic beam. We can see the knocked up component of deuteron distribution appears almost the same direction as energetic protons.

Next the deuteron distribution function is evaluated by solving 2D FP equation. The knocked up deuteron distribution previously obtained (see Fig. 6) is used as a source term for FP equation. The knocked up deuterons are produced and slow down via Coulomb collisions with background ions and electrons continuously. The equilibrium distribution can be thus obtained by solving the FP equation. The equilibrium deuteron distribution functions are shown in Fig. 7 corresponding to (a) tangential and (b)

Table 2  ${}^6\text{Li}(d,\gamma){}^7\text{Li}$  reaction rate coefficients and the degree of the enhancement compared with the values of Maxwellian plasmas for several beam injection energies.

$E_{\text{NBI}}$ [keV]	$\langle\sigma v\rangle_{6\text{Li}+d}$ [ $\text{m}^3/\text{s}$ ]	$\eta$
100	$5.3\times 10^{-33}$	1.34
200	$5.2\times 10^{-31}$	130
300	$5.1\times 10^{-30}$	1295
400	$2.6\times 10^{-29}$	6496
500	$5.5\times 10^{-29}$	13746

vertical proton injections shown in Fig. 5. By using the deuteron distribution function obtained, we can evaluate the  ${}^6\text{Li}(d,\gamma){}^7\text{Li}$  reaction rate coefficient from Eq. (7). For the velocity distribution function shown in Fig. 7 (a) the  ${}^6\text{Li}(d,\gamma){}^7\text{Li}$  reaction rate coefficient is  $5.18\times 10^{-31}\text{ m}^3/\text{s}$ , while for Fig. 7 (b)  $5.35\times 10^{-31}\text{ m}^3/\text{s}$ , we cannot see meaningful discrepancy between tangential and vertical beam injections. When Maxwellian is assumed for both deuteron and  ${}^6\text{Li}$  velocity distribution functions, the reaction rate coefficient is evaluated as  $3.93\times 10^{-33}\text{ m}^3/\text{s}$  in this condition. It is found that the reaction rate coefficient is enhanced approximately 2 orders of magnitude as a result of knock-on tail formation. The similar simulations are made for various beam injection energies for tangential injection, and the results are summarized in Table 2. Here the  $\eta$  represents the ratio of the  ${}^6\text{Li}(d,\gamma){}^7\text{Li}$  reaction rate coefficients compared with the values for Maxwellian plasmas, i.e.,  $\eta \equiv \langle\sigma v\rangle_{6\text{Li}+d} / \langle\sigma v\rangle_{6\text{Li}+d}^{\text{Maxwellian}}$ . As the beam injection energy increases, the cross section of NES increases and the energy range where the knock-on tail is created also shifts to the high-energy range. This accelerates the enhancement of the  ${}^6\text{Li}(d,\gamma){}^7\text{Li}$  reaction rate coefficient. It is found that if protons are injected to plasmas with 500 keV energy, the 0.48-MeV  $\gamma$ -ray generation rate increases approximately 4 orders compared with the value for Maxwellian plasma.

We next look at the radial profile of the 0.48-MeV  $\gamma$ -ray generation rate. The similar analyses described in the previous paragraph are carried out for every radial position in a Tokamak plasma. We consider the situations that protons are born at 30 cm from the magnetic axis toward tangential and vertical directions, and 15 cm toward vertical direction with 200 keV beam-injection energy (see Fig. 8). Radial profiles of normalized proton density are shown in Fig. 9. The proton density peaks at the position where protons generate, and broadened to both sides in the radial direction. The proton distribution functions at 25, 30, 35 and 40 cm from the magnetic axis when proton beam is injected toward vertical direction with 200 keV energy at 30 cm from the magnetic axis are shown in Fig. 10. For

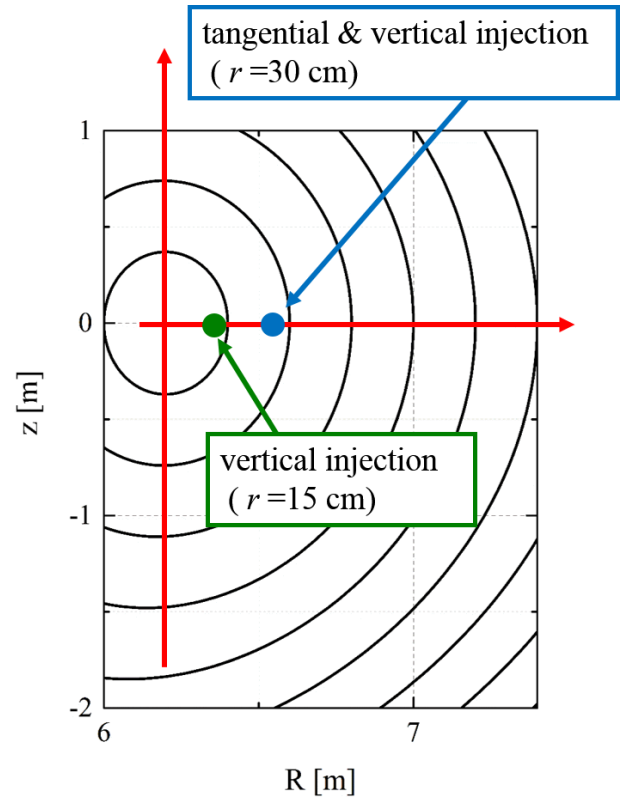


Fig. 8 Schematic view of the proton generation points in Tokamak device.

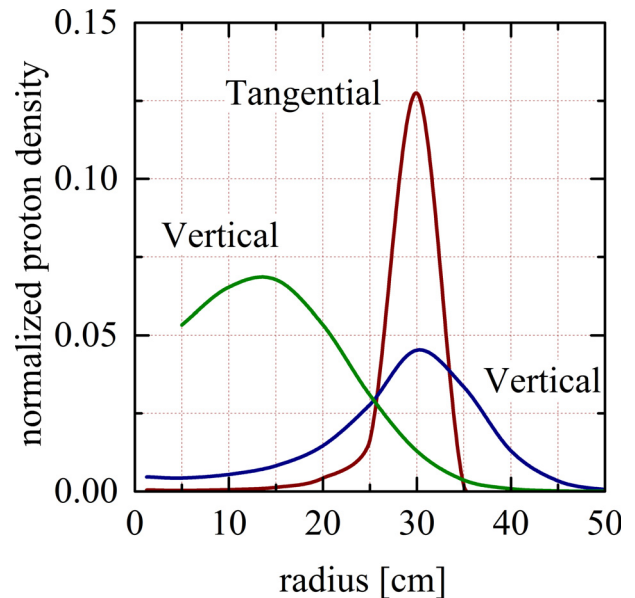


Fig. 9 Radial profiles of normalized proton density for several calculation conditions. Deuteron density  $n_d(0) = 10^{19}\text{ m}^{-3}$ , electron temperature  $T_e(0) = 2\text{ keV}$  and beam-injection energy  $E_{\text{NBI}} = 200\text{ keV}$  are assumed.

every position the similar calculations shown previously are made. We can see that the non-Maxwell component is largest at the point where protons generate, i.e., 30 cm.

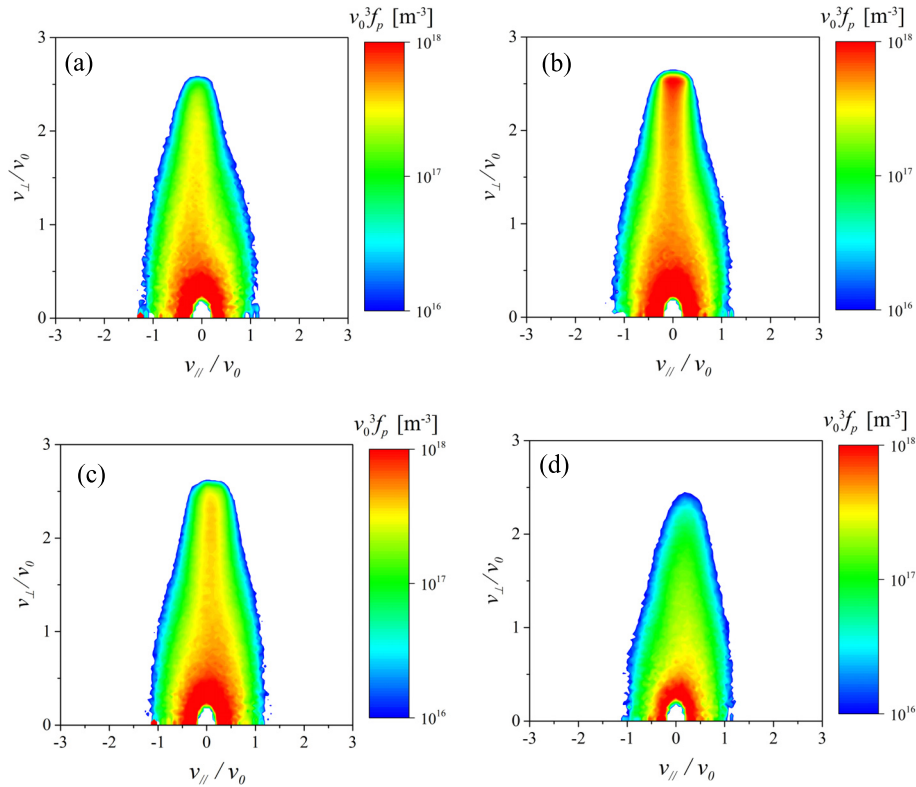


Fig. 10 Proton velocity distribution functions at (a) 25, (b) 30, (c) 35 and (d) 40 cm positions from the magnetic axis when protons generate at 30 cm point with 200-keV beam-injection energy toward vertical direction. Deuteron density  $n_d(0) = 10^{19} \text{ m}^{-3}$  and electron temperature  $T_e(0) = 2 \text{ keV}$  are assumed.

The  ${}^6\text{Li}(d,\gamma){}^7\text{Li}$  reaction rate coefficients are 5.3, 34.1, 13.0 and  $0.79 \times 10^{-30} \text{ m}^3/\text{s}$  at 25, 30, 35 and 40 cm positions respectively. The radial profiles of the 0.48-MeV  $\gamma$ -ray emission rate are shown in Fig. 11 as a function of the minor radius from the magnetic axis when protons are born at 30 cm toward tangential and vertical directions, and at 15 cm toward vertical direction. The radial profiles of the  $\gamma$ -ray emission rate are almost the same shape with the radial profile of the proton density. The total 0.48-MeV  $\gamma$ -ray emission rate from the plasma is summarized as almost  $3.7 \times 10^8$  for all cases shown in Fig. 11, which is consistent the result obtained by using volume-averaged proton distribution function.

So far we have assumed a point source of the protons in the plasma, which implies that all of the injected hydrogens are ionized at a spatial point in the plasma as a monoenergetic beam. Actually the neutral hydrogens, however, are ionized with a spatial profile along with the beam injection line. The effect can be considered by superposing the results of the point source which is discussed in the previous paragraphs. Here as an example, the radial profile of the reaction rate coefficient of the  ${}^6\text{Li}(d,\gamma){}^7\text{Li}$  reaction is examined and the results are shown in Fig. 12 considering ionization profile. In the calculation 200-keV proton beam injected with tangential direction to the toroidal axis on the horizontal plane is considered. The white bars repre-

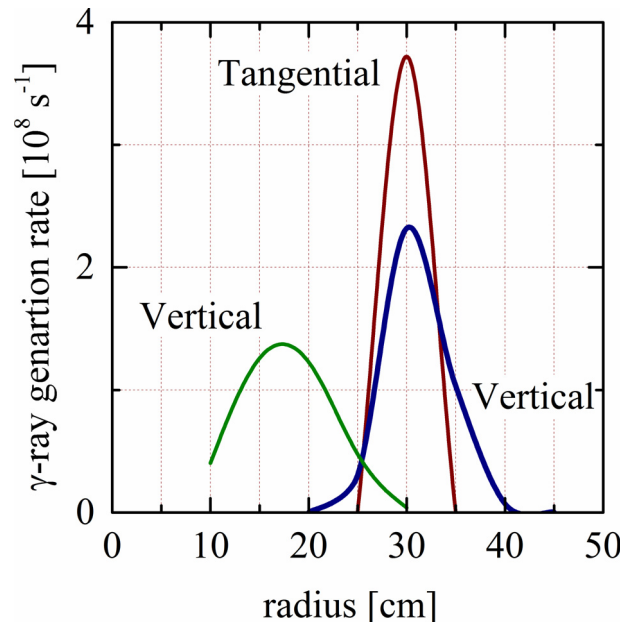


Fig. 11 Radial profiles of 0.48-MeV  $\gamma$ -ray emission rate for several beam-injection conditions. Deuteron density  $n_d(0) = 10^{19} \text{ m}^{-3}$ ,  ${}^6\text{Li}$  density  $n_{{}^6\text{Li}}(0) = 10^{17} \text{ m}^{-3}$ , electron temperature  $T_e(0) = 2 \text{ keV}$  and beam-injection energy  $E_{\text{NBI}} = 200 \text{ keV}$  are assumed.

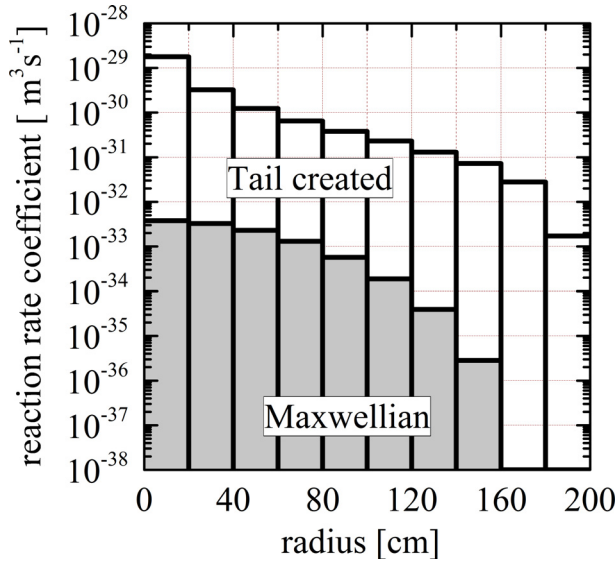


Fig. 12 Radial profiles of reaction rate coefficient of 0.48-MeV  $\gamma$ -ray generation ( ${}^6\text{Li}(d,\text{p}){}^7\text{Li}$ ) reaction when considering neutral hydrogen ionization profile. Deuteron density  $n_d(0) = 10^{19} \text{ m}^{-3}$ , electron temperature  $T_e(0) = 2 \text{ keV}$  and beam-injection energy  $E_{\text{NBI}} = 200 \text{ keV}$  are assumed.

sent the rate coefficient when knock-on tail is considered, while the shading bars denote the ones when Maxwellian plasma is assumed. An attenuation of the neutral hydrogen beam is simulated considering ionization reactions with background deuterons and electrons, and charge exchange reaction with deuterons. In this case the most of the hydrogens are ionized near the center region in the poloidal plane. This is because the traveling length of the hydrogen beam in the plasma is longer in the center region. Thus the knock-on tail in the deuteron distribution function also grows large near the center region. We can see that the rate coefficient rapidly increases at the center region. On the other hands since the background deuteron density decreases and most of the ionized protons are easily lost from the plasma at outer plasma region, the rate coefficient becomes small in the region. In addition, the temperature also rapidly decreases at the outside region, and especially when Maxwellian plasma is assumed, the rate coefficient is significantly reduced at the outer region.

In Fig. 13 we next show the radial profiles of the 0.48-MeV  $\gamma$ -ray generation rate when knock-on tail is considered and not considered (Maxwellian). The calculation conditions are the same as those in Fig. 12. We can see a peak at the 20-40 cm layer. This is because the plasma volume of each region becomes smaller with decreasing minor radius. The total 0.48-MeV  $\gamma$ -ray generation rate over whole plasma region is estimated as  $2.5 \times 10^8 \text{ s}^{-1}$ . The value is almost 30% smaller compared with the point source simulation (Fig. 11). This is because in the point source simulation, penetration loss of the neutral hydro-

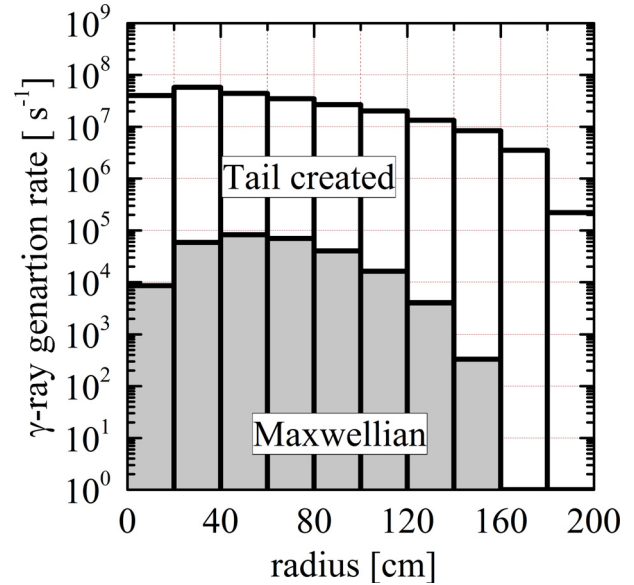


Fig. 13 Radial profiles of 0.48-MeV  $\gamma$ -ray emission rate when considering neutral hydrogen ionization profile. Deuteron density  $n_d(0) = 10^{19} \text{ m}^{-3}$ ,  ${}^6\text{Li}$  density  $n_{{}^6\text{Li}}(0) = 10^{17} \text{ m}^{-3}$ , electron temperature  $T_e(0) = 2 \text{ keV}$  and beam-injection energy  $E_{\text{NBI}} = 200 \text{ keV}$  are assumed.

gens is not considered in the estimation. In addition, since protons exist inner region of the plasma, the decrement of the temperature and densities, and the proton loss at the outer region of the plasma are not included. In the simulation shown in Figs. 12 and 13, almost 30% of hydrogens are lost from the plasma.

Throughout the calculations the energy confinement time has been assumed as  $\tau_E = 1 \text{ sec}$ . With decreasing energy confinement time, relative intensity of the energetic to thermal component increases. This is because the energy loss due to thermal conduction is mainly carried out by bulk component. Thus for small confinement time the reaction rate coefficient (0.48-MeV  $\gamma$ -ray generation rate) tends to be enhanced further significantly. On the other hands if the confinement time increases, the enhancement of the rate coefficient would be reduced.

#### 4. Concluding Remarks

The enhancement of the 0.48-MeV  $\gamma$ -ray emission rate via  ${}^6\text{Li}(d,\text{p}){}^7\text{Li}$  reactions due to NES by energetic protons is examined using the newly-developed analysis model considering ion behavior in Tokamak magnetic configuration. It is shown that the 0.48-MeV  $\gamma$ -ray emission rate considerably changed according to the magnitude of the knock-on tail in deuteron distribution function, and it can be a useful tool to examine the knock-on tail formation for various plasma conditions.

The results obtained by the present model, i.e., total 0.48-MeV  $\gamma$ -ray emission rate from the plasma, are almost

the same as those by previous 1-D BFP model. By using the present model, however, radial profile of the emission rate for several plasma condition can be evaluated in addition to the total emission rate, i.e., more detailed comparison can be possible in the future experiment using deuterium plasmas. In the present model, the proton distribution is evaluated by the ion trajectory analysis, however, the distribution function once obtained is fixed in the subsequent knock-on tail simulation process. As a result of the energy transfer process from energetic protons to bulk deuterons via NES, i.e., knock-on tail formation, the proton distribution itself is also expected to slow down. The current treatment tends to a little bit overestimate the magnitude of the knock-on tail.

In this paper we only show the possibility for the use of the  $\gamma$ -ray generating  ${}^6\text{Li}(d,p\gamma){}^7\text{Li}$  reaction to examine the knock-on tail formation due to NES. To compare the simulations with experimental data, much plenty of simulations for various plasma conditions would be required. The radial profile of NBI energy deposition and penetration should be well discussed and an optimal experimental conditions should be determined. With reference to the relevant information, a scenario to grasp the NES effect should be clarified. There may be other endoergic reactions which can be used for the observation of the knock-on tail in addition to the  ${}^6\text{Li}(d,p\gamma){}^7\text{Li}$  reaction. The subsequent investigation for the other useful reactions and a possible scenario for the future experiment are our next issues.

## Acknowledgments

The authors acknowledge Prof. R.B. White for providing ORBIT code. The first author acknowledges Prof. Y. Nakao, Prof. O. Mitarai, Prof. T. Johzaki and Prof. T. Takahashi for continuous discussions and encouragements for research of NES effects in burning plasmas. Special thanks also go to Mr. D. Uchiyama for fruitful discussions about coordinate transformation technique in the present

simulation model.

- [1] L. Ballabio, G. Gorini and J. Källne, *Phys. Rev. E* **55**, 3358 (1997).
- [2] J. Källne, L. Ballabio, J. Frenje *et al.*, *Phys. Rev. Lett.* **85**, 1246 (2000).
- [3] J.J. Devany and M.L. Stein, *Nucl. Sci. Eng.* **46**, 323 (1971).
- [4] S.T. Perkins and D.E. Cullen, *Nucl. Sci. Eng.* **20**, 77 (1981).
- [5] H. Matsuura and Y. Nakao, *Phys. Plasmas* **13**, 062507 (2006).
- [6] H. Matsuura and Y. Nakao, *Phys. Plasmas* **14**, 054504 (2007).
- [7] H. Matsuura *et al.*, *Plasma Phys. Control. Fusion* **53**, 035023 (2011).
- [8] H. Matsuura *et al.*, *Proc. ICENES'93* (Chiba, 1993), edited by H. Yasuda (World Scientific, Singapore, 1994) p.266.
- [9] Y. Nakao *et al.*, *Fusion Technol.* **27**, 555 (1995).
- [10] M. Nakamura *et al.*, *J. Phys. Soc. Jpn.* **75**, 024801 (2006).
- [11] Y. Nakao *et al.*, *Nucl. Fusion* **21**, 979 (1981).
- [12] J. Galambos *et al.*, *Nucl. Fusion* **24**, 739 (1984).
- [13] Y. Nakao *et al.*, *Nucl. Fusion* **28**, 1029 (1988).
- [14] J.F. Clarke, *Nucl. Fusion* **20**, 563 (1980).
- [15] H. Matsuura *et al.*, *Plasma Fusion Res.* **7**, 2403076 (2012).
- [16] H. Matsuura *et al.*, *Plasma Fusion Res.* **2**, S1078 (2007).
- [17] H. Matsuura *et al.*, *Fusion Sci. Technol.* **60**, 634 (2011).
- [18] H. Matsuura *et al.*, *Plasma Fusion Res.* **8**, 2403064 (2013).
- [19] V.T. Voronchev, V.I. Kukulkin and Y. Nakao, *Phys. Rev. E* **63**, 26413-1 (2001).
- [20] V.T. Voronchev *et al.*, *Mem. Fac. Eng. Kyushu Univ.* **51**, 63 (1991).
- [21] A.J. Elwyn *et al.*, *Phys. Rev. C* **16**, 1744 (1977).
- [22] S.N. Abramovich *et al.*, *Bull. Kazakh Acad. Sci. Phys. Math.* **4**, 24 (1984).
- [23] R.B. White *et al.*, *Phys. Fluids* **27**, 2455 (1984).
- [24] V.A. Yavorskij *et al.*, *Plasma Phys. Control. Fusion* **43**, 249 (2001).
- [25] B.J. Green, *Plasma Phys. Control. Fusion* **45**, 687 (2003).
- [26] E. Bittoni, J.G. Cordey and M. Cox, *Nucl. Fusion* **20**, 931 (1980).
- [27] J.G. Cordey *et al.*, *Nucl. Fusion* **14**, 441 (1974).